

## **Efficient 3D data compression through parameterization of free-form surface patches**

RODRIGUES, Marcos <<http://orcid.org/0000-0002-6083-1303>>, ROBINSON, Alan and OSMAN, Abdulsslam

Available from Sheffield Hallam University Research Archive (SHURA) at:

<https://shura.shu.ac.uk/5195/>

---

This document is the

**Citation:**

RODRIGUES, Marcos, ROBINSON, Alan and OSMAN, Abdulsslam (2011). Efficient 3D data compression through parameterization of free-form surface patches. In: Signal Process and Multimedia Applications (SIGMAP), Proceedings of the 2010 International Conference on. IEEE, 130-135. [Book Section]

---

**Copyright and re-use policy**

See <http://shura.shu.ac.uk/information.html>

# EFFICIENT 3D DATA COMPRESSION THROUGH PARAMETERIZATION OF FREE-FORM SURFACE PATCHES

Marcos A Rodrigues, Alan Robinson and A. Osman

*Geometric Modelling and Pattern Recognition Research Group, Sheffield Hallam University, Sheffield, UK  
m.rodrigues@shu.ac.uk, a.robinson@shu.ac.uk, a8039462@my.shu.ac.uk*

Keywords: 3D data compression, surface parameterization, 3D reconstruction

Abstract: This paper presents a new method for 3D data compression based on parameterization of surface patches. The technique is applied to data that can be defined as single valued functions; this is the case for 3D patches obtained using standard 3D scanners. The method defines a number of mesh cutting planes and the intersection of planes on the mesh defines a set of sampling points. These points contain an explicit structure that allows us to define parametrically both  $x$  and  $y$  coordinates. The  $z$  values are interpolated using high degree polynomials and results show that compressions over 99% are achieved while preserving the quality of the mesh.

## 1 INTRODUCTION

Cheap storage and secure transmission of 3D data bring advantages to a number of applications in security, engineering, CAD/CAM collaborative design, medical visualization, entertainment and e-commerce among others. We have developed and demonstrated original methods and algorithms for fast 3D scanning for a number of applications with particular focus on security (Robinson, 2004), (Brink, 2008), (Rodrigues, 2008), (Rodrigues, 2009). Our algorithms can perform 3D reconstruction in 40ms and recognition in near real-time, in just over one second per subject.

This paper is concerned with compression of 3D data for fast transmission over the Internet. A realistic scenario we are exploring involves 3D facial biometric verification at airports. The method is non-intrusive and aims at minimal disruption and is based on our past experience with 3D biometrics at Heathrow Airport (London, UK) in 2005. An enrollment shot is taken and reconstructed in 3D at an automated check-in desk, where a new database is created for each flight. At the gate, before boarding the plane another 3D shot is taken for verification. The created databases are transmitted to the local Police who would perform a search against their records. If the Police find no information to warrant keeping the data for longer, all data must be erased after a time

lapse, normally within 24 hours. For international flights and where no mechanisms for sharing information between Police Forces are available, the data can be transmitted to the destination Police authorities *before* the flight actually arrives at the destination.

A significant constraint of this scenario is that 3D files are very large; a high definition 3D model of a person's face is around 20MB. For a flight with 400 passengers, this would mean to dispatch 8GB of data. If we consider the number of daily flights in a medium sized airport, we soon conclude that this may be unworkable. It is clear that methods to compress 3D data would be beneficial to the scenario considered here but, more importantly, would represent an enabling technology for a potential large number of other applications.

Although some standards exist for 3D compression such as Java 3D and MPEG4, the compression rates are still low for general sharing of files over the Internet. In general there are three methods one can use to share 3D data. The first method is based on image compression where each snapshot of a 3D scene is compressed as a 2D image. The second method is based on hierarchical refinement of a 3D structure for transmission, where a coarse mesh is followed by increasing refinements until the original, full 3D model is reconstructed at the other end. The third method is based on mesh compression where algorithms tra-

verse the mesh for local compression of polygonal relationships.

Compression methods are focused on representing the connectivity of the vertices in the triangulated mesh. Examples include the Edgebreaker algorithm (Szymczak, 2000) and (Szymczak, 2002). Products also exist in the market that claim a 95% lossless file reduction such as from 3D Compression Technologies Inc (3DCT, 2010) for regular geometric shapes. Other techniques for triangulated models include the work of (Shikhare, 2002) and vector quantization based methods (Hollinger, 2010) where rates of over 80:1 have been achieved.

The 3D compression method proposed in this paper was devised from our research on fast 3D acquisition using light structured methods (Robinson, 2004), (Rodrigues, 2008), (Brink, 2008), (Rodrigues, 2009). The 3D scanning method is based on splitting the projection pattern into light planes. Each plane hits the target object as a straight line and the apparent bending of the light due to the position of the camera in relation to the projection allows us to calculate the depth of any point along the projected light plane. Taking full advantage of such properties, our method is closer to polygonal mesh compression but with significant differences as it does not depend on searching for local relationships that are most susceptible to compression. We have achieved compression rates of free-form surface patches that drastically reduce the original 3D data by over 99% to a plain text file. Once in plain text, it can be encrypted and securely transmitted over the network and reconstructed at the other end.

This paper is organized as follows. Section 2 presents the method and Section 3 describes the instantiation of the method to surface patches. The data are compressed and reconstructed and a comparative analysis of polynomials of various degrees is provided. Finally a conclusion is presented in Section 4.

## 2 METHOD

### 2.1 The Surface Patch as an Explicit Function of Two Variables

The method presented here applies to surface patches acquired by standard 3D scanning techniques. Any such patch can be described as a single valued shape in one dimension where their values are represented as an explicit function of two independent variables. The height of a point is represented by their  $z$ -value and we can say that the height of a function  $(x, y)$

is some function  $f(x, y)$ . The advantage of a single-valued function is that it has a simple parametric form,

$$P(u, v) = (u, v, f(u, v)) \quad (1)$$

with normal vector  $\mathbf{n}(u, v) = (-\delta f / \delta u, -\delta f / \delta v, 1)$ . Both  $u$  and  $v$  are the dependent variables for the function and  $u$ -contours lie in planes of constant  $x$ , and  $v$ -contours lie in planes of constant  $y$ . When such patch is visualized in 3D using quads, each edge of the polygons is a trace of of the surface cut by a plane with  $x = k_1$  and  $y = k_2$  for some values of  $k_1$  and  $k_2$ .

### 2.2 Sampling and Reconstruction

Given a randomly oriented surface patch described in relation to a global coordinate system, it is necessary to orient the surface using the properties of its bounding box. Geometric algorithms exist to approximate a minimum bounding box of a 3D object defined by a set of points, e.g. (Lahanas, 2010). The patch must be rotated until its minimum bounding box edges are aligned with the  $x$ -,  $y$ -, and  $z$ -axes of the global coordinate system. Normally, the smallest dimension of the bounding box is aligned with the  $z$ -axis. The proposed method is based on sampling surface points at the intersection of horizontal and vertical mesh cutting planes.

Horizontal and vertical planes are defined as parallel to one of the  $x$  or  $y$ -axes with normal vectors  $(1, 0, 0)$  and  $(0, 1, 0)$  respectively. The intersection of any two planes defines a line, and the points where such lines intersect the mesh are sampled. A problem here is that we cannot guarantee that the intersection of two planes on the mesh will rest on a vertex. More likely, it will intersect somewhere on a polygon's face somewhere between vertices. A good approximation is to find the three vertices on the mesh that are the nearest to the intersection line. Such vertices define a plane and it then becomes straightforward to determine the intersection point. Assume that the line has a starting point  $S$  and direction  $\mathbf{c}$ . The intersection line is given by

$$L(t) = S + \mathbf{c}t \quad (2)$$

The solution only involves finding the intersection point with the generic plane (Hill, 2001). The generic plane is the  $xy$ -plane or  $z = 0$ . The line  $S + \mathbf{c}t$  intersects the generic plane when  $S_z + \mathbf{c}_z t_i = 0$  where  $t_i$  is  $t$  "intersection":

$$t_i = -\frac{S_z}{c_z} \quad (3)$$

From equation (2), the line hits the plane at point  $P_i$ :

$$P_i = S - \mathbf{c} \left( \frac{S_z}{c_z} \right) \quad (4)$$

The vector of all points on the mesh belonging to a particular plane is a sub-set of the sampled points. Depending on the characteristics of the surface patch, either the set of points lying in the horizontal or vertical planes can be selected. If the selected points lie in planes with normal vector  $(1,0,0)$ , the distance between each sampled point is the distance between planes with normal  $(0,1,0)$  and vice-versa. Calling these distances  $D_1$  and  $D_2$ , the  $x$  and  $y$  coordinates of any sampled point can be recovered for all planes  $k$ :

$$x_r = \{rD_1, |r = 1, 2, \dots, k_1\} \quad (5)$$

$$y_c = \{cD_2, |c = 1, 2, \dots, k_2\} \quad (6)$$

where  $(r,c)$  are the indices of the planes. This is a significant outcome of the proposed method, as it is not necessary to save the actual values  $(x,y)$  of each vertex; instead, only  $D_1, D_2, k_1$  and  $k_2$  are kept. This allows us to discard 2/3 of the data. To illustrate the compactness of this representation, a mesh with 100,000 vertices means that we have to keep 300,000 values for the set  $(x,y,z)$ . We instantly eliminated 200,000 values replacing them by 4 numbers only.

We now turn our attention to the  $z$ -values. These can be expressed as in equation (1) as a single valued function and estimated using equation (4) for each combination of  $(x_r, y_c)$ . If we choose to represent these as the set of points belonging to planes with normal  $(1,0,0)$  this is reduced to a 2D case in which on the horizontal axis we have exactly  $k_2$  points with constant step of  $D_2$  and on the vertical axis we have their corresponding  $z$ -values. This can be expressed as an  $n$ -th-degree polynomial in  $z$

$$a_0 + a_1z + a_2z^2 + \dots + a_nz^n \quad (7)$$

A high degree polynomial fitting is performed on each of such curves using the  $z$ -values as ‘‘control points’’. The desired outcome is a polynomial that passes *exactly* through each control point. The coefficients of the polynomial are saved for each curve together with the indices of the  $k$  planes for the first and last valid vertices. This is so because we may have several plane intersections that do not intersect the mesh and such combination of indices  $(k_r, k_c)$  must be marked as invalid vertices.

The reduction in data is substantial: using the earlier example of 100,000 vertices, if we cut the mesh with 100 planes we need to keep a set of 100 polynomial coefficients together with the first and last valid vertex indices. Assuming that we are using a polynomial of degree 25, we need to keep 28 numbers for each plane: 26 coefficients plus 2 vertex indices. This is a reduction from 100,000 to 2,800 numbers. To reconstruct the original mesh, the polynomials used in equation (7) are evaluated for each plane within their

boundaries (first and last valid vertices), and the  $(x,y)$  values are evaluated for each combination of  $(r,c)$  plane indices through equations (5) and (6).

### 3 RESULTS

In this section we describe a step by step application of the method described in Section 2 with comparative analysis of interpolation using various high degree polynomials.

#### 3.1 Data Compression

The steps and the parameters used for data compression are as follows.

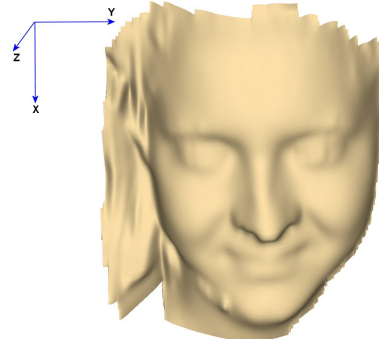


Figure 1: Original 3D mesh with 48,672 vertices and 78,043 faces. The size of the file (OBJ format) is 4.83MB with texture mapping and 4.0MB with no texture.

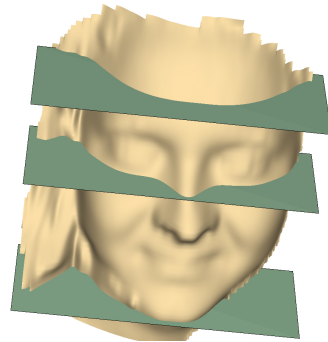


Figure 2: 72 horizontal planes with normal  $n = (1,0,0)$  are cut through the mesh, from top to bottom (only 3 are shown here).

1. A given triangulated surface patch acquired using a structured light scanner is aligned to the global coordinate system where the smallest dimension of its bounding box is aligned with the  $z$ -axis (Figure 1).

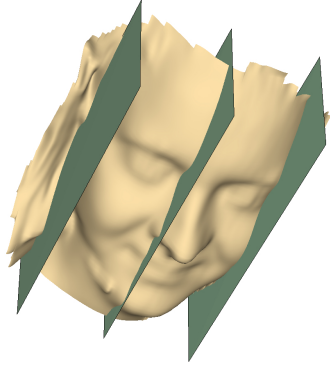


Figure 3: 676 vertical planes with normal  $n = (0, 1, 0)$  are cut through the mesh, from left to right (only 3 are shown here).



Figure 4: The intersection points of each horizontal and vertical planes on the mesh are estimated and marked with a point in red. The shown model has 39,743 valid vertices or intersection points.

2. A number  $k_1$  of horizontal planes with normal  $\mathbf{n} = (1, 0, 0)^T$  cut the mesh as shown in Figure 2 (only 3 planes are shown). These planes are parallel to the Y-Z plane of the coordinate system in Figure 1.
3. A number  $k_2$  of vertical planes with normal  $\mathbf{n} = (0, 1, 0)^T$  cut the mesh as shown in Figure 3 (only 3 planes are shown). These planes are parallel to the X-Z plane of the coordinate system.
4. The intersection of each plane  $k_r$  with plane  $k_c$  defines a line. For each line determine the point  $P_{r,c}$  where the line intersects the mesh through equation (4). These are the heights of the single-valued function.
5. For each plane  $k_r, k_c$  make a list of the intersection points  $P_{r,c}$ .
6. The distance between each horizontal plane is defined as a constant  $D_1$  and the distance between vertical planes is defined as a constant  $D_2$ .

7. Perform polynomial interpolation and save the coefficients and the plane indices of the first and last valid points.

Figure 4 depicts the intersection of all horizontal and vertical planes where each intersection is marked with a red point. The structure of the mesh is  $k_1 \times k_2$ , whose choice depends on the characteristics of the model and the accuracy required. For the face models, we normally chose 8 to 10 times more vertical planes than horizontal ones due to the characteristics of our scanner (Robinson, 2004). Ultimately, the number of planes is based on experience; we determined that between 50–80 horizontal planes across the face provide for good reconstruction. The number of vertical planes was determined at around 10 times the horizontal scale; this provides a large number of data points for polynomial interpolation and results in a grid  $72 \times 676$  for the face model shown (for different models these dimensions can vary or remain the same). The horizontal planes are quite noticeable in the picture, while the vertical planes are less so due to their proximity.

A polynomial interpolation is suggested of degree 20 or higher as we wish to find a polynomial that goes as close as possible through all control points. In order to be able to reconstruct the set of points later on, we save together with each set of coefficients the first and last valid points of each list of points, the size  $k_1, k_2$  of the sampled 3D data structure and the distance between planes  $D_1$  and  $D_2$ . This information is organized in the file header:

```
k1 72
k2 676
D1 3.3
D2 0.3
8.0960151e-031 ... 6.7726253e+002 382 482
...
1.8712059e-032 ... 1.0464188e+007 143 437
```

### 3.2 3D Reconstruction

Reconstruction is achieved by evaluating the polynomials from the saved information. In the example above, the 4 lines of header information are followed by 72 lines of polynomial coefficients with their first and last valid points. The degree of the polynomial is inferred from the data. If each line has say, 23 numbers, the last two numbers are the indices of the first and last valid points, leaving the preceding 21 numbers as polynomial coefficients  $C$ . The degree of the polynomial is  $C - 1$  thus, the data was interpolated with a polynomial of degree 20.

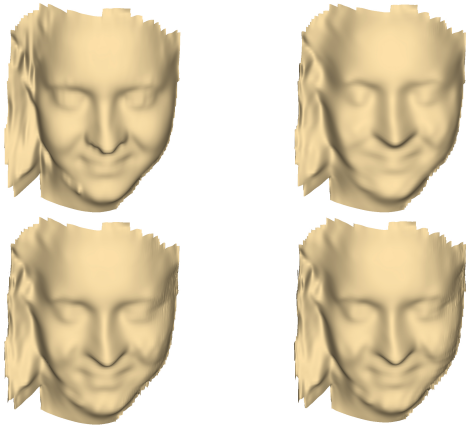


Figure 5: Top row: the original face model is shown on the left with file size of 4MB; right, with polynomial interpolation of degree 20 reducing the file size to 26KB. Bottom row: left, polynomial interpolation of degree 30 reducing the file size to 37.2KB; right, degree 40 reducing to 48.5KB.

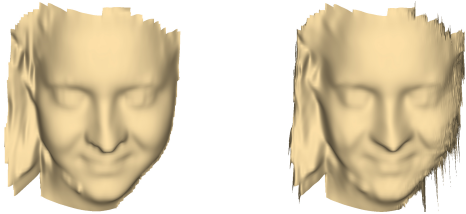


Figure 6: Left, the original face model; right, interpolation with polynomial degree 80. It is noted that the model becomes unstable.

Figure 5 show results for polynomial interpolation of degrees 20, 30, and 40. Figure 6 shows the original face model on the left together with a compression and reconstruction with a polynomial of degree 80. It is noted that the model becomes unstable for interpolation of very high degrees. For a polynomial interpolation of degree 20, the file size in OBJ format has been reduced from 4MB to 26KB. This is a reduction of 99.35% and similar reductions were achieved for other polynomials also; a summary is presented in Table 1.

### 3.3 Evaluating the Fit

Determining the quality of a polynomial regression or how well the recovered data points fit the original data can involve a number of tests including statistics summaries. By far the most meaningful way is by plotting the original and regression data sets and visually assess its quality. By visually analyzing the models of Figure 5, it is suggested that a polynomial interpolation of degrees 20 to 40 describes well the data and

Table 1: Compression rates in percentage.

Degree	20	30	40	50	80
Rate	99.35	99.07	98.79	98.53	97.66

can be well-suited for most applications.

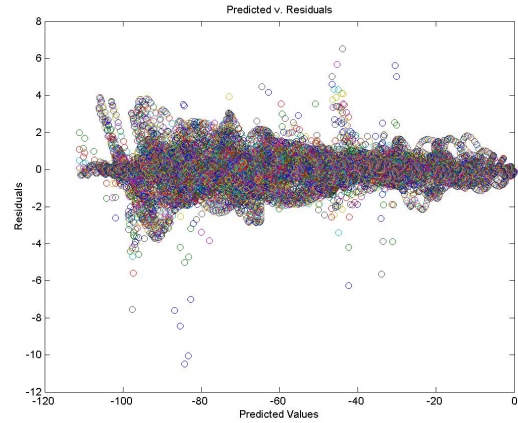


Figure 7: Scatter plot of Predicted Values against Residuals. For a good fit, it should show no patterns and no trends. The plot shows what looks like random noise indicating a good fit.

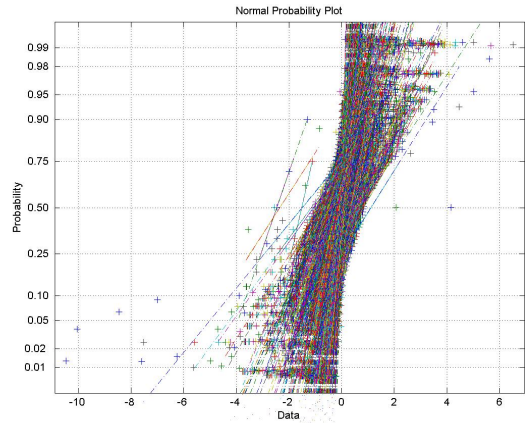


Figure 8: The normal-probability plot of the residuals. A good fit should describe a straight line for each polynomial curve which is verified by the plot indicating a good fit.

Another way of assessing quality is to look at the residuals and plot them against the predicted values. Figure 7 shows the plot for data interpolated with a polynomial of degree 30. For a good fit, the plot should display no patterns and no trends. The scatter plot shows what looks like random noise which is a good measure of the quality of the fit. Alternatively, if

the fit is good, a normal-probability plot of the residuals should display a straight line. The plot depicted in Figure 8 shows that for most polynomials evaluated at each plane, indeed they describe a straight line indicating a good fit.

There are a number of statistical measures to assess the quality or the appropriateness of a model such as the coefficient of determination also known as  $R^2$  that indicates the percent of the variation in the data that is explained by the model. This can be estimated by first calculating the deviation of the original data set which gives a measure of the spread. While the total variation to be accounted for (SST) is given by the sum of deviation squared, the variation that is *not* accounted for is the sum of the residuals squared (SSE). The variation in the data explained by the model is given by

$$R^2 = 1 - \frac{SSE}{SST} \quad (8)$$

expressed as percentage. The  $R^2$  values for some interpolated models are described in Table 2. The table shows a trend of increasing  $R^2$  as the polynomial degree increases, peaking at around degree 30. For higher degrees,  $R^2$  decreases monotonically, and this is also confirmed by visual inspection of the 3D reconstructed models whose quality deteriorates as they become unstable for high degree polynomials.

Table 2: The coefficients of determination  $R^2$  for polynomial fits of degrees 20–80 for the given data.

Degree	20	30	40	50	80
$R^2$	0.9995	0.9996	0.9995	0.9994	0.9909

## 4 CONCLUSIONS

We have presented a new method of data compression applied to surface patches that can be defined as a single valued function. This is the case of 3D data acquired using standard 3D scanning technologies. The method was described based on mesh cutting planes oriented with the global coordinate system with constant step. The points where the plane intersections intersect the mesh are sampled and this automatically allows the recovery of all  $(x,y)$  coordinates for all vertices. The  $z$ -values are subject to polynomial interpolation of various degrees. Results demonstrate that the method is effective and can reduce the mesh over 99%. Both close visual inspection and statistical measures demonstrate that optimal performance is achieved for polynomials of degree between 20 to 40 – it seems that the optimal value is around 30, but this obviously depends on the characteristics of the data.

There seems to be intrinsic limitations using polynomials to approximate complex real world surface patches. In the future we will investigate the use of splines as it is possible to get more accurate results than with polynomials but the price we pay is that it will generate larger files as we need to keep the coefficients of all polynomials between the control points. A more promising approach is to investigate the use of PDEs and research is under way and will be reported in the near future.

## REFERENCES

- 3DCT (2010). 3D Compression Technologies Inc. available at <http://www.3dcompress.com/web/default.asp>
- Brink, W., A. Robinson, and M. Rodrigues (2008). Indexing Uncoded Stripe Patterns in Structured Light Systems by Maximum Spanning Trees, *British Machine Vision Conference BMVC 2008*, Leeds, UK, 1–4 Sep 2008
- Hill, F.S. Jr (2001). *Computer Graphics Using OpenGL*, 2nd edition, Prentice-Hall Inc, 922pp.
- Hollinger, S.Q., A.B. Williams, and D. Manak (2010). 3D data compression of hyperspectral imagery using vectorquantization with NDVI-based multiple codebooks, available at <http://sciencestage.com>
- Lahanas, M. (2010). Optimal Oriented Bounding Boxes, [http://www.mlahanas.de/CompGeom/opt\\_bbox.htm](http://www.mlahanas.de/CompGeom/opt_bbox.htm), last accessed April 2010.
- Rodrigues, M.A. and A. Robinson (2010). Novel Methods for Real-Time 3D Face Recognition, *6th Annual International Conference on Computer Science and Information Systems*, 25–28 June 2009, Athens, Greece.
- Rodrigues, M.A., A. Robinson, and W. Brink (2008). Fast 3D Reconstruction and Recognition, in *New Aspects of Signal Processing, Computational Geometry and Artificial Vision*, 8th WSEAS ISCGAV, Rhodes, 2008, p15–21.
- Robinson, A., L. Alboul and M.A. Rodrigues (2004). Methods for Indexing Stripes in Uncoded Structured Light Scanning Systems, *Journal of WSCG*, 12(3), 2004, pp 371–378.
- Szymczak, A., D. King and J. Rossignac (2000). An Edgebreaker-Based Efficient Compression Scheme for Regular Meshes, *12th Canadian Conference on Computational Geometry*, pp 257–265.
- Szymczak, A., J. Rossignac, and D. King (2002). Piecewise Regular Meshes, *Graphical Models* 64(3-4), 2002, 183–198.
- Shikhare, D., S.V. Babji, and S.P. Mudur (2002). Compression techniques for distributed use of 3D data: an emerging media type on the internet, *15th international conference on Computer communication*, India, pp 676–696.